Proof-of-concept of polymetallic phyto-extraction of base metal mine tailings from Queensland, Australia

Philip Nti Nkrumah (p.nkrumah@uq.edu.au)
Centre for Mined Land Rehabilitation, Sustainable Minerals Institute, The University of Queensland
https://orcid.org/0000-0003-1437-4305

Amelia Corzo Remigio
The University of Queensland, Queensland, Australia

Antony van der Ent
The University of Queensland, Queensland, Australia

Research Article

Keywords: hyperaccumulator plants, elemental distribution, metal uptake, metal demand, mine tailings, polymetallic

Posted Date: March 10th, 2022

DOI: https://doi.org/10.21203/rs.3.rs-1421198/v1

Abstract

Purpose The increasing volumes of mine tailings that are being generated globally because of the rise in metal demand whilst ore-grades continue to decline call for novel sustainable management options. Phytoextraction using hyperaccumulator plant species may be one of such strategies. However, base metal mine tailings are inherently polymetallic that necessitate targeting multiple metal(loid)s for effective phytoextraction. The aim of this study was to conduct a proof-of-concept for polymetallic phytoextraction of base metal mine tailings.

Methods Selected hyperaccumulator plants (*Noccaea caerulescens* targeting zinc, *Biscutella laevigata* and *Silene latifolia* targeting thallium, *Phytolacca octandra* targeting manganese) were grown in monocultures and mixed cultures for 12 weeks on tailings from the zinc-lead Dugald River and Mt Isa Mines, Queensland, Australia.

Results *Noccaea caerulescens* accumulated zinc and manganese (up to ~1 wt% and ~1.4 wt%, respectively) with zinc-manganese co-localization at the leaf apex and margins. The monocultured *B. laevigata* exhibited severe toxicity symptoms, which were alleviated when co-cultured with *N. caerulescens*. Trichomes were important storage sites for zinc and manganese in *B. laevigata*. *Silene latifolia* accumulated higher thallium than *B. laevigata,* whilst *P. octandra* promoted thallium accumulation in *S. latifolia.*

Conclusions This proof-of-concept test of polymetallic phytoextraction provides a real-life demonstration of this innovative technology which could be adapted to base metal mines around the world.

Introduction

Global demand for metallic elements is surging because of the technological shift required for a net-zero carbon emission transition (European Commission 2020; IEA 2021; Mudd 2020; Xu et al. 2020). Base metal mining occurs around the world, with Australia being a major producer of lead (Pb), zinc (Zn), copper (Cu), silver (Ag) and nickel (Ni) (Mudd et al. 2017; Spitz and Trudinger 2019). There are > 70 major base metal mines/fields across Australia (Mudd 2007). One of the most significant production centres are the Mt Isa deposits in northwest Queensland, which have the largest reserves of Pb, Zn and Ag in the world (Williams 1998) and hosts some of the leading global producers of base metals, including the Mt Isa Mines and Dugald River Mine. The Mt Isa Mines commenced production in 1931 (Mudd 2007), whereas the Dugald River Mine became operational in 2017 (Creus et al. 2021). The tailings material generated from base metal mining generally contains high concentrations of potentially toxic trace elements, including arsenic (As), cadmium (Cd) and thallium (Tl). Large volumes of this potentially hazardous material is generated as ore-grades continue to decline whilst metal demand and production surge (Jowitt et al. 2020; Mudd 2020). Mine tailings management is one of the major issues confronting the mining industry, governments, and the society at large, with deleterious repercussions on the environment and public health if inappropriately managed (Entwistle et al. 2019). Environmentally

friendly and cost-effective approaches are required to holistically address the increasing risk of tailings contamination from active and abandoned mines. However, in many mine tailings, their inherent geochemical characteristics present strong challenges for effective rehabilitation.

Hyperaccumulator plants have the unique ability to tolerate and accumulate high concentrations of potentially toxic trace elements into their shoots (Reeves 2003). Notional threshold values in dry shoot matter for recognition of hyperaccumulation are set at 100 μg g^{-1} for Cd, selenium (Se) and Tl; 300 μg g^{-1} for cobalt (Co) and Cu; 1000 μg g^{-1} for As and nickel (Ni); 3000 μg g^{-1} for Zn; and 10,000 μg g^{-1} for manganese (Mn) (van der Ent et al. 2013). On this basis, there are currently 746 hyperaccumulator species known globally: 532 Ni, 53 Cu, 42 Co, 42 Mn, 41 Se, 20 Zn, seven Cd, five As, two Tl, and two rare earth elements (REEs) (Reeves et al. 2018a,b). Hyperaccumulation has both fundamental (*e.g.*, ion homeostasis in plants) and applied (*e.g.*, phytoextraction and biofortification) importance (Chaney and Baklanov 2017; Clemens 2017; van der Ent et al. 2015, 2017).

Phytoextraction involves the *in situ* cultivation of selected hyperaccumulator plants on a metal-rich substrate followed by subsequent harvesting and processing of the metal-rich biomass to recover valuable metal(loid)s and/or to remove hazardous elements from their biomass for safe disposal (Anderson et al. 1999; Nkrumah et al. 2016, 2018, 2019). Phytoextraction can be cost-effective and environmentally friendly and potentially generate economic gains from valuable metals, such as Ni, Co, and Tl from unconventional resources such as mine tailings (Corzo Remigio et al. 2020; van der Ent et al. 2021). Production of high-purity metal salts from the harvested biomass may in the future partly meet the growing demand for critical metals required for the global net-zero carbon emission transition (Nkrumah et al. 2022). The main limitation of phytoextraction is the number of known hyperaccumulator plant species with the right combination of desirable traits including high biomass production and a high accumulation capacity for the target element (Nkrumah et al. 2021). Furthermore, hyperaccumulator plant species typically tolerate and accumulate only one or two elements simultaneously (van der Ent et al. 2019). This presents a problem at many metal-contaminated sites, including base metal mine tailings, because they are intrinsically polymetallic. The Dugald River Mine tailings have high Mn, Zn, Cd, Tl and Pb concentrations, whilst the Mt Isa Mine tailings also have high Cu, Co, As and Tl concentrations, but lower Zn and Mn concentrations (Forsyth et al. 2015; Huang et al. 2015; Tang et al. 2021). Another difference between these sites is that the tailings from the Dugald River Mine are not yet weathered because they have only recently been produced, and this may have an effect on the phytoavailable metal concentrations. Considering the inherent polymetallic characteristics of these tailings, as well as other base metal mine tailings around the world, it may not be useful to target single metal(loid) during phytoextraction. However, this drawback may be overcome by selecting a purposeful assemblage of hyperaccumulator plant species that in concert tolerate and accumulate multiple metal(loid)s thereby providing synergistic conditions for optimum growth and metal yield of all cultivated species.

Substantial unrealised opportunities exist in Australia for the discovery of hyperaccumulator plant species considering the high level of plant diversity and widespread metalliferous soils (Abubakari et al. 2021a,b; Lottermoser et al. 2008). However, the majority of the limited local hyperaccumulator plant

species discovered so far either produce low biomass or are very slow growing and therefore, not suitable for economic phytoextraction (Batianoff et al. 1990; Bidwell et al. 2002; Fernando et al. 2009; Severne 1974). Recent field surveys have led to the discovery of Australian native species that may have greater potential. This includes the finding of one of the strongest Se hyperaccumulator plant species known in the world, *Neptunia amplexicaulis* (Fabaceae) endemic to Central Queensland, which may open new opportunities for a Se phytoextraction industry in regional Australia (Harvey et al. 2020). In addition, the discovery of the polymetallic (Zn-Cu-Cd) hyperaccumulator *Crotalaria novae-hollandiae* (Fabaceae) from the Dugald River gossan may find applications in phytoremediation and possibly phytoextraction in Australia (Tang et al. 2021).

Elucidating elemental distribution at the organ, tissue, cellular or subcellular levels can provide insights into the mechanisms underlying the high tolerance and accumulation physiologies in these species (van der Ent et al. 2018). Synchrotron and laboratory-based micro-X-ray fluorescence technology permits mapping of a wide range of elements in plant organs and tissues (van der Ent et al. 2021). Information on elemental distribution coupled with elemental concentrations and growth data could aid in developing improved hyperaccumulator cultivars and optimising the agronomic parameters required for practical phytoextraction (Broadhurst et al. 2009; van der Ent et al. 2017). For example, the co-localization of Ni and Mn in the leaf tissues of *Odontarrhena* (*Alyssum*) species (Brassicaceae) suggests that employing this species for Ni phytoextraction on Mn-rich soils may affect Ni yields (Broadhurst et al. 2009).

This study aims to investigate the responses of model polymetallic hyperaccumulator plants to typical polymetallic tailings and to provide a proof-of-principle for polymetallic phytoextraction on Zn-Pb base metal mine tailings from Australian mines. Some of the species used in this study will not be suitable for application in the semi-arid tailings in Central Queensland. However, it is hoped that the proof-of-concept may ultimately be adopted employing local native species if they are discovered.

Materials And Methods

Plant species – The selected model species included *Noccaea caerulescens* (Brassicaceae) targeting zinc, *Biscutella laevigata* (Brassicaceae) and *Silene latifolia* (Caryophyllaceae) targeting thallium, *Phytolacca octandra* (Phytolaccaceae) targeting manganese, and *Pityrogramma calomelanos* (Pteridaceae) targeting arsenic. Furthermore, we employed the well-known metal tolerant species capable of producing root exudates, *Lupinus albus* (Fabaceae). The intensively studied hyperaccumulator *N. caerulescens* from Europe has the ability to hyperaccumulate Ni, Zn, Pb and Cd with accessions differing in their ability to tolerate and accumulate (Assunção et al. 2003; Deng et al. 2014; Gonneau et al. 2014; Schwartz et al. 2003). The level of bioconcentration in *N. caerulescens* is extreme as it can accumulate up to 52,000 µg g^{-1} foliar Zn (Zhao et al. 2003), whilst it can also attain 3410 µg g^{-1} foliar Cd (Reeves et al. 2001, 2018a,b). *Biscutella laevigata* can attain > 3 wt% foliar Tl when growing on soils with ~ 400 µg Tl g^{-1} (Pošćić et al. 2015) and *S. latifolia* up to 1500 µg Tl g^{-1} (Escarré et al. 2011). *Pityrogramma calomelanos* is an As hyperaccumulator that can reach up to 8350 µg As g^{-1} in its fronds (Francesconi et al. 2002). *Phytolacca octandra* and *L. albus* produce root exudates, thereby increasing phytoavailable

metal concentrations (Dinkelaker et al. 1989; Lambers et al. 2015). Moreover, *Phytolacca* species are Mn hyperaccumulators and may be beneficial in reducing Mn-toxicity to co-cultivated plants *via* the removal of available Mn from the rhizosphere (Pollard et al. 2009). Phytoavailability of the target metal(s) in the soil or substrate is a key consideration for the effectiveness of phytoextraction (Nkrumah et al. 2016, 2021) and we hypothesize that co-cultivating root exudates-producing plants with selected model hyperaccumulator plants could increase metal accumulation, especially in relatively low phytoavailable metal substrates. Finally, as a legume, *L. albus* is a nitrogen-fixing species which may improve the fertility of the substrate for the co-cultivated hyperaccumulator plants.

Experimental design – The seed accession of *N. caerulescens* (Navacelles, France, non-metalliferous) was chosen purposely because it has a particularly high bioconcentration factor for Zn (Escarré et al. 2000). The seed accessions of *B. laevigata* and *S. latifolia* originated from Saint-Laurent-le-Minier, Southern France (metalliferous). Seeds of *P. octandra* were collected near Brisbane, Australia, while seeds of *L. albus* were purchased from a commercial supplier in Brisbane and *Pityrogramma calomelanos* sporelings were collected from north Queensland. The experiments were conducted in plastic boxes (45 × 30 × 12 cm, L, W, H) in which a 1 cm layer of plastic granules (for irrigation) was covered by a plastic mesh and then filled with tailings mixes consisting of 90:5:5 and 75:10:15 (w/w/w) tailings/peat moss/perlite for Dugald River Mine and Mt Isa Mine tailings, respectively. The Dugald River Mine tailings have chemical properties that are generally amenable to plant growth (pH 6.75, relatively low salinity), although it has high concentrations of Mn (0.41 wt%), Zn (22,000 mg kg^{-1}), Cd (50 mg kg^{-1}), Tl (30 mg kg^{-1}), Pb (8220 mg kg^{-1}). The Mt Isa Mine tailings had relatively lower Mn (0.17 wt%), Zn (10,100 mg kg^{-1}), Cd (35 mg kg^{-1}), Pb (6240 mg kg^{-1}), but higher Tl (75 mg kg^{-1}). Seeds of *N. caerulescens*, *B. laevigata* and *S. latifolia* were germinated separately on Gelzan gel in 2 mL Eppendorf tubes (made from 0.5-strength Hoagland's solution). The seeds were then vernalized for one week at 3°C and acclimatized for four days at 26°C (van der Zee et al. 2021). Seeds of *P. octandra* were treated with sulphuric acid for 15 mins and rinsed with ultrapure water before sowing in a 1:1 mix of perlite and vermiculite. The seedlings (approx. 1 cm in size) were transplanted to the boxes. Four treatments with 16 biological replicates were undertaken on the Dugald River Mine substrate: *B. laevigata* only, *B. laevigata* + *N. caerulescens*, *B. laevigata* + *L. albus* and *N. caerulescens* only. In addition, seven treatments with 16 biological replicates were undertaken on the Mt Isa Mine substrate: *B. laevigata* only, *B. laevigata* + *P. calomelanos*, *B. laevigata* + *L. albus*, *N. caerulescens* only, *B. laevigata* + *P. octandra*, *S. latifolia* only and *S. latifolia* + *P. octandra*. The plants were grown for a total period of 12 weeks, harvested and then separated into root and shoot fractions for analysis as described below.

Bulk analysis of plant tissue samples – All of the plant material samples were thoroughly washed with demineralised water and then oven dried at 70°C for 3 days. The samples were weighed and then ground to a fine powder in an impact mill at 15,000 rpm (IKA Tube Mill 100 control with disposable titanium blades) and then 100 ± 5 mg of each sample was weighed into 6 mL polypropylene tubes. The samples were pre-digested using 2 mL HNO_3 (70%) for 24 hr before digestion in a block heater (Thermo Scientific™ digital dry bath) for a 2-hr programme (1 hr at 70°C followed by 1 hr at 125°C). The digestates were then

brought to volume (10 mL) with ultrapure water before analysis with Inductively coupled plasma atomic emission spectroscopy (ICP-AES) with a Thermo Scientific iCAP 7400 instrument for macro-elements (Mg, P, S, K, Ca) and trace-elements (Mn, Fe, Cu, Zn, As, Cd, Tl, Pb) in radial and axial modes depending on the element and expected analyte concentration. All elements were calibrated with a 4-point curve covering analyte ranges in the samples.

Collection and analysis of tailings samples – Samples of the respective substrates collected from 5–20 cm depth were air-dried and sieved through a 630 µm screen. The pH was measured in a 1:2.5 substrate to water slurry after 2 hr mixing on an end-over-end shaker and a 1-hr rest. Sub-samples were weighed (100 ± 5 mg) in quartz digestion vessels and 5 mL HNO_3 (70%) and 2 mL HCL (37%) were added. The samples were then digested for 15 min at 80% power using a ColdBlock system (CB15S 15 channel system, ColdBlock Technologies Inc) which uses high-intensity infrared irradiation to aid rapid acid digestion (Wang et al. 2014). The digestates were quantitatively transferred to 50 mL tubes, brought to volume (40 mL) and filtered (Whatman® Grade 1 filter paper) before analysis with ICP-AES.

micro-X-ray fluorescence elemental mapping – The UQ micro-XRF facility is a custom-built system manufactured by IXRF which consists of two 50 kV sources (1000 µA) fitted with polycapillary focussing optics: XOS microfocus Mo-target tube producing 17.4 keV X-rays (flux of 2.2×10^8 ph s^{-1}) focussing to 25 µm and a Rh-target tube producing 20.2 keV (flux of 1.0×10^7 ph s^{-1}) focussing to 5 µm. The system is fitted with two silicon drift detectors (SDD) of 150 mm^2 coupled to a XIA Mercury X4 signal processing unit. The fresh foliar samples were mounted between two sheets of 4 µm Ultralene thin film in a tight sandwich to limit evaporation and analysed within 10 minutes after excision. The mounted samples between Ultralene thin film were stretched over a Perspex frame magnetically attached to the x-y motion stage at atmospheric temperature (~ 20°C). The UQ microXRF facility acquired the XRF spectra in mapping mode using the instrument control package, Iridium (IXRF systems), from the sum of counts at the position of the principal peak for each element. They were then exported into ImageJ as greyscale 8-bit TIFF files, internally normalised such that each image covered the full dynamic range and displayed using ImageJ's "Fire" lookup table.

Statistical analyses

Statistical analyses were performed using OriginPro 2021 (https://www.originlab.com/). The elemental concentrations of the plant fractions were presented in Tables and plotted in Figures as mean ± standard error. Significant differences were determined by ANOVA, separated by Tukey's honestly significant difference (HSD) test ($p < 0.05$) and indicated by different letters.

Results

Growth performance on the mine tailings

Noccaea caerulescens grew well in all treatments (Fig. 1), but the biomass on the Mt Isa Mine substrate was significantly higher than that on the Dugald River Mine substrate ($p < 0.05$) (Fig. 2D). On the Dugald River Mine substrate, the biomass of the monoculture treatment was not significantly different from the treatment co-cultured with *B. laevigata* ($p > 0.05$). For *B. laevigata*, the growth was significantly reduced on the Dugald River Mine substrate, except when co-cultured with *N. caerulescens* (Fig. 1F, G, H, 3D). The plants in the Mt Isa Mine substrate grew well irrespective of the type of culture and the biomass production was similar to that co-cultured with *N. caerulescens* in the Dugald River Mine substrate ($p > 0.05$). The *S. latifolia* grew well in the Mt Isa substrate in both the monoculture treatment and co-culture with *P. octandra* and did not differ significantly from the biomass of *B. laevigata* growing on a similar substrate ($p > 0.05$) (Fig. 4D). *Lupinus albus* grew well in the Mt Isa Mine substrate but showed severe toxicity symptoms in the Dugald River Mine substrate (Fig. 1). *Phytolacca octandra* and *P. calomelanos* grew well in the Mt Isa Mine tailings.

Elemental accumulation by N. caerulescens **and** B. laevigata

Noccaea caerulescens accumulated higher Mn and Zn concentrations in the Dugald River Mine substrate compared to the Mt Isa Mine substrate (> 10-fold, $p < 0.05$) (Fig. 2, Table 1). On the Dugald River Mine substrate, the Mn and Zn concentrations in the monoculture treatment were significantly higher than when co-cultured with *B. laevigata* (> 3-fold; $p < 0.05$). *Biscutella laevigata* accumulated higher Tl concentrations on the Mt Isa Mine substrate than that on the Dugald River Mine substrate (> 3-fold, $p < 0.05$) (Fig. 3A, Table 1). However, an opposite pattern to foliar Tl was observed for foliar Mn and Zn concentrations in the respective substrates (Fig. 3). In the Dugald River Mine substrate, the Mn and Zn concentrations in the monoculture treatment were significantly higher than that co-cultured with *N. caerulescens* (Fig. 3B, C). Co-culture with *P. octandra* significantly increased Tl concentrations in *S. latifolia* ($p < 0.05$), whereas the effect on Mn and Zn concentrations was not significant ($p > 0.05$) (Fig. 4, Table 1). *Phytolacca octandra* accumulated considerable concentrations of Mn, Fe, Cu, Zn and Cd, whereas Mn and As were the only trace elements accumulated in relatively higher concentrations by *L. albus* and *P. calomelanos*, respectively (Table 1). For the macro elements, *B. laevigata* and *P. calomelanos* accumulated relatively higher P compared to *P. octandra* (Table 1b). *Lupinus albus* and *P. octandra* had relatively lower K concentrations compared to *B. laevigata* (~ 2-fold, $p < 0.05$). *Biscutella laevigata* accumulated significantly higher Ca than all the other species ($p < 0.05$).

Table 1

a Foliar elemental concentrations in mg kg^{-1} (trace elements) in the respective treatments. There were 16 plants per box. Mean ± standard error for each element followed by the same letter are not significantly different ($p > 0.05$) according to the Tukey test. *** deceased plants*.

Substrate	Treatments	Mn	Fe	Cu	Zn	As	Cd	Tl	Pb
Dugald River Mine	***B. laevigata* only**	11 300 ± 755 a	320 ± 70 a	10 ± 2.0 bc	14 700 ± 940 a	0.45 ± 0.05 b	85 ± 8.85 ab	20 ± 1.45 cde	30 ± 4.5 cd
	B. laevigata (+ *N. caerulescens*)	4260 ± 520 b	95 ± 7.0 bc	3.9 ± 0.4 c	3370 ± 285 c	0.15 ± 0.05 b	20 ± 2.15 cde	20 ± 2.35 cde	60 ± 8.5 bc
	***B. laevigata* (+ *L. albus*)**	6420 ± 775 b	300 ± 70 a	7.9 ± 1.3 bc	11,700 ± 1100 b	0.25 ± 0.05 b	55 ± 9.5 bc	10 ± 0.99 cde	9.0 ± 1.5 d
	*** L. albus* (+ *B. laevigata*)**	4980 ± 725 b	180 ± 65 abc	6. 5 ± 1.5 bc	9690 ± 1520 b	0.25 ± 0.10 b	35 ± 9.5 cde	5.5 ± 0.95 de	8.5 ± 2.5 d
	N. caerulescens (+ B. laevigata)	1770 ± 450 c	180 ± 20 abc	6.5 ± 0.7 bc	3500 ± 825 c	0.50 ± 0.10 b	60 ± 15 bc	20 ± 15 cde	80 ± 20 b
	N. caerulescens only	5870 ± 470 b	195 ± 20 ab	10 ± 0.7 bc	10,200 ± 495 b	0.55 ± 0.05 b	110 ± 10 a	6.15 ± 0.45 e	130 ± 10 a
Mt Isa Mine	*B. laevigata* only	530 ± 65 c	95 ± 8.0 bc	8.5 ± 1.5 bc	490 ± 130 d	1.10 ± 0.10 b	5.70 ± 3.11 e	90 ± 10 bc	10 ± 2.0 d
	B. laevigata (+ *L. albus*)	545 ± 95 c	90 ± 9.0 bc	8.5 ± 1.6 bc	380 ± 50 d	1.15 ± 0.15 b	2.1 ± 0.25 de	95 ± 10 abcd	9.5 ± 1.5 d
	B. laevigata (+ *P. calomelanos*)	370 ± 70 c	65 ± 7.0 bc	7.5 ± 2.0 bc	375 ± 55 d	0.85 ± 0.05 b	1.2 ± 0.19 e	130 ± 35 ab	10 ± 1.5 d
	L. albus (+ *B. laevigata*)	1100 ± 145 c	35 ± 2.0 c	5.8 ± 0.5 c	320 ± 45 d	0.55 ± 0.05 b	1.0 ± 0.15 e	0.96 ± 0.12 e	3.0 ± 0.25 d

Substrate	Treatments	Mn	Fe	Cu	Zn	As	Cd	Tl	Pb
	P. calomelanos (+ *B. laevigata*)	100 ± 20 c	205 ± 65 abc	11 ± 2.0 bc	140 ± 30 d	35 ± 7.5 a	0.80 ± 0.07 e	8.25 ± 2.45 de	10 ± 4.65 d
	N. caerulescens only	255 ± 30 c	120 ± 10 bc	6.9 ± 0.4 c	900 ± 150 d	1.05 ± 0.15 b	35 ± 7.9 cd	2.45 ± 0.30 e	10 ± 1.70 d
	P. octandra (+ *B. laevigata*)	590 ± 105 c	165 ± 20 abc	100 ± 5.6 a	3370 ± 185 c	0.35 ± 0.20 b	50 ± 2.0 bc	25 ± 4.5 cde	9.5 ± 2.25 d
	P. octandra (+ *S. latifolia*)	1150 ± 240 c	215 ± 25 ab	115 ± 15 a	2530 ± 235 cd	0.80 ± 0.10 b	50 ± 6.0 bc	30 ± 2.25 cde	10 ± 0.85 d
	S. latifolia only	620 ± 130 c	190 ± 25 abc	20 ± 1.5 bc	550 ± 55 d	0.90 ± 0.15 b	0.60 ± 0.09 e	55 ± 10 bcde	10 ± 1.20 d
	S. latifolia (+ *P. octandra*)	665 ± 165 c	285 ± 25 a	25 ± 1.5 b	315 ± 50 d	2.5 ± 0.25 b	1.5 ± 0.25 e	180 ± 65 a	30 ± 3.0 cd

Table 1

b Foliar elemental concentrations in g kg^{-1} (macro elements) in the respective treatments. There were 16 plants per box. Mean ± standard error for each element followed by the same letter are not significantly different ($p > 0.05$) according to the Tukey test. *** deceased plants*.

Substrate	Treatments	Mg	P	S	K	Ca
Dugald River Mine	***B. laevigata* only**	19 ± 1.5 bcd	3.0 ± 0.2 efg	55 ± 5.3 a	49 ± 3.2 abc	16 ± 1.0 cd
	B. laevigata (+ *N. caerulescens*)	10 ± 0.6 efg	3.5 ± 0.3 cdef	14 ± 1.3 cd	45 ± 2.6 abcd	26 ± 2.0 b
	***B. laevigata* (+ *L. albus*)**	10 ± 1.0 cdefg	2.7 ± 0.2 efgh	32 ± 4.4 b	35 ± 2.6 bcdef	11 ± 0.9 defg
	*** L. albus* (+ *B. laevigata*)**	9.5 ± 1.5 efg	3.0 ± 0.4 defg	31 ± 4.7 b	26 ± 3.1 efg	5.0 ± 0.6 g
	N. caerulescens (+ B. laevigata)	7.9 ± 1.8 fg	4.3 ± 0.5 bcde	11 ± 1.5 cd	46 ± 3.7 abcd	15 ± 2.0 cde
	N. caerulescens only	11 ± 0.6 efg	5.0 ± 0.3 abc	12 ± 0.5 cd	54 ± 3.2 a	13 ± 0.6 defg
Mt Isa Mine	*B. laevigata* only	21 ± 1.8 b	4.6 ± 0.4 bcd	20 ± 1.5 bc	34 ± 1.6 de	21 ± 1.5 bc
	B. laevigata (+ *L. albus*)	21 ± 2.5 b	6.0 ± 0.5 ab	18 ± 0.8 bcd	40 ± 3.6 bcde	26 ± 2.6 b
	B. laevigata (+ *P. calomelanos*)	10 ± 0.5 efg	6.4 ± 0.8 a	13 ± 0.9 cd	39 ± 2.9 bcde	35 ± 2.5 a
	L. albus (+ *B. laevigata*)	10 ± 1.1 defg	1.6 ± 0.1 fgh	12 ± 1.4 cd	20 ± 2.4 fg	6.5 ± 0.8 fg
	P. calomelanos (+ *B. laevigata*)	6.9 ± 0.8 g	6.0 ± 0.6 ab	7.8 ± 0.9 d	35 ± 1.9 cde	13 ± 2.5 defg
	N. caerulescens only	7.5 ± 1.5 g	2.5 ± 0.1 fg	7.1 ± 1.9 d	29 ± 1.5 efg	7.9 ± 0.6 efg
	P. octandra (+ *B. laevigata*)	19 ± 3.0 bcde	0.7 ± 0.05 h	14 ± 1.1 cd	16 ± 2.0 g	12 ± 1.5 defg
	P. octandra (+ *S. latifolia*)	40 ± 1.9 a	1.2 ± 0.05 gh	30 ± 1.9 b	19 ± 2.4 g	12 ± 1.3 defg
	S. latifolia only	20 ± 2.1 bc	1.8 ± 0.2 fgh	10 ± 1.3 d	29 ± 2.5 efg	14 ± 1.8 def
	S. latifolia (+ *P. octandra*)	17 ± 2.7 bcdef	3.1 ± 0.4 defg	16 ± 2.9 cd	51 ± 3.0 ab	8.2 ± 1.0 defg

Micro-XRF analysis of foliar elemental distribution

In *N. caerulescens* Zn was strongly enriched in the margin, with excess distributed in the lamina, whereas the midrib and the veins were particularly depleted (Fig. 5). Similarly, Mn was enriched in margin, but depleted in midrib, veins, and lamina. In contrast, K was enriched in the midrib, veins and lamina but depleted in the margin. Calcium was enriched in the lamina but depleted in the midrib, veins, and margin. For *B. laevigata*, Zn was primarily in the midrib and veins, with excess stored in the base of the trichomes (Figs. 6, 7). However, the lamina and the margin were much lower in Zn. This pattern of Zn distribution is opposite to that of *N. caerulescens*. Manganese was mainly stored in the trichomes, with excess distributed to the margin and tips. However, the midrib and the veins were depleted in Mn. Thallium was distributed primarily in the midrib and margin, with excess in the veins. However, the lamina and the trichomes were depleted in Tl. The trichome rays were enriched in Ca compared to the trichome base, lamina, and veins. Potassium was enriched in the midrib and lamina but depleted in the tips and trichome rays (Fig. 6).

For *P. octandra*, Zn was enriched in the lamina, but depleted in the midrib, veins, and tip, opposite to the pattern observed for K (Fig. 8). Manganese was enriched in the margin compared to the lamina. The midrib and the veins were particularly depleted in Mn. Calcium was enriched in the lamina and leaf margins but depleted in the midrib and veins. For *L. albus*, Zn was depleted in the lamina but relatively enriched in the midrib, veins, and margin (Fig. 9). Manganese was enriched in the margin but depleted in the midrib, veins, and lamina. A similar distribution pattern was observed for Ca but that of K was opposite. For *P. calomelanos*, Zn and K were enriched in the rachis and pinna but depleted in the pinnules; an opposite distribution pattern was observed for Ca (Fig. 9).

Discussion

Noccaea caerulescens performed well in all of the treatments in the Dugald River Mine and Mt Isa Mine substrates, including substrates with relatively higher Mn and Zn concentrations, and accumulated these metals at high concentrations in its leaves (reaching ~ 1 wt% Mn and ~ 1.4 wt% Zn) (Figs. 1, 2, Table 1). This finding shows that *N. caerulescens* is highly tolerant to elevated Mn and Zn and is a prime candidate for phytoextraction on these substrates. The elemental maps reveal co-localization of Mn and Zn (together with Ca) in the leaf tips and margins (Fig. 5), suggesting similar storage mechanisms (Callahan et al. 2016). However, limited research exists on Zn distribution in *N. caerulescens* at the whole leaf level (Callahan et al. 2016; do Nascimento et al. 2021) as opposed to that at the cellular and sub-cellular levels (Küpper et al. 1999). Recent evidence suggests that the Zn distribution in whole leaves of *N. caerulescens* may be accession dependent (van der Zee et al. 2021), with some accessions accumulating Zn in the cells surrounding the central and secondary veins (do Nascimento et al. 2021), and other accessions storing Zn at the leaf tip (Callahan et al. 2016). The Mn localization in the margins of *N. caerulescens* is consistent with that of the Mn hyperaccumulator *P. octandra* (Fig. 8), Mn hypertolerant *L. albus* (Fig. 9; Blamey et al. 2018) and several other Mn hyperaccumulator plants, including *Gossia bidwillii*, *G. fragrantissima*, *Denhamia bilocularis*, *D. silvestris* and *P. americana* (Abubakari et al. 2021a,b, 2022; Xu et al. 2006). The Mn localization in the margins of these species is attributed to increasing transpiration

rates closer to leaf margins which result in greater Mn accumulation in leaf marginal areas (Abubakari et al. 2021a,b).

The monocultured *B. laevigata* in the high Mn and Zn substrate (Dugald River Mine) exhibited severe toxicity symptoms (Fig. 1G). The elemental maps show preferential accumulation of elevated Zn in the base of the trichomes, similar to that of *Arabidopsis halleri* and sunflower (Küpper et al. 2000; Li et al. 2019, 2021; Sarret et al. 2009). The movement of excess Zn into the base of trichomes, likely into cell wall, lowers the Zn concentrations in the remainder of the leaf, which is an important Zn detoxification mechanism (Li et al. 2019, 2021). It is likely that continued Zn loading, in excess of trichome base storage capacity, of the monocultured *B. laevigata* on the Dugald River Mine substrate increased the Zn concentrations in the remainder of the leaf, thereby partly contributing to its toxicity (Fig. 6). Future dosing trials could test the Zn concentration threshold at which toxicity starts in *B. laevigata*. In addition, time-resolved µ-XRF techniques could clarify the mechanism of Zn toxicity in *B. laevigata*, as has been demonstrated for Mn toxicity in soybean and sunflower (van der Ent et al. 2020). The storage of Mn in trichomes is an important detoxification mechanism for several Mn hypertolerant plants (Blamey et al. 1986, 2015; Broadhurst et al. 2009; McNear and Küpper 2014). Excess Mn in the trichomes due to continued Mn loading starts to accumulate in the apoplastic space or walls of the surrounding cells, as observed in *Odontarrhena chalcidica* (*Alyssum murale*) and sunflower (Blamey et al. 1986, 2015; McNear and Küpper 2014). This mechanism may partly explain the toxicity symptoms in the monocultured *B. laevigata* in the Dugald River Mine substrate. However, the *B. laevigata* plants co-cultured with *N. caerulescens* on the high Mn and Zn substrate did not show any toxicity symptom. It is possible that *N. caerulescens* reduced Mn and Zn availability to *B. laevigata* (Fig. 7). Moreover, the monoculture *B. laevigata* grown in the Mt Isa Mine substrate did not experience any toxicity symptom partly because all the Mn safely accumulated in the trichomes, whilst Zn safely accumulated in the midrib and veins (Fig. 6).

Conclusions

A major drawback with phytoextracting a targeted metal from polymetallic substrate is that there may be other non-targeted metals that may be toxic to the selected hyperaccumulator plants, in a process described as ‘co-metallic effect’ (Anderson et al. 2013). The discovery of a communalistic relationship at least in terms of growth for these model hyperaccumulator plants overcomes this drawback, and suggests that, in principle, it may be possible to tailor-make a purposeful assemblage of hyperaccumulators for any polymetallic substrate. The facilitation of metal accumulation in selected hyperaccumulators by root-exudates producing species is also worth investigating further. We suggest that this nature-based metal phytoavailability enhancement may provide an alternative to the use of cost prohibitive and environmentally hazardous synthetic chelates such as ethylene diamine tetraacetic acid (EDTA) (Grčman et al. 2001; Meers et al. 2005; Nowack et al. 2006). The relatively low foliar concentrations of Fe, Cu, As, Pb show the ability of the model species to biopurify the target metals, which enhances the metal recovery process. The production of high purity metal salts could partly meet

the growing demand for battery metals (Nkrumah et al. 2022). The findings in this study provide baseline information for developing *in situ* polymetallic phytoextraction of base metal mines.

Declarations

ACKNOWLEDGEMENTS

We kindly acknowledge Lachlan Casey (Centre for Microscopy and Microanalysis, The University of Queensland) for assistance with the laboratory μ-XRF analysis. We thank the AMMRF at the Centre for Microscopy and Microanalysis at the University of Queensland for their support in the microanalysis. We thank Fuyao Chen and Roger H. Tang for assistance with the experiments. We also thank MMG Limited for supplying the Dugald River Mine tailings.

FUNDING

This research was funded by the Queensland Department of Natural Resources, Mines and Energy project “Extracting Queensland’s Rare Earth Elements Sustainably” and the Sustainable Minerals Institute (UQ) Complex Orebodies strategic initiative program. Amelia Corzo Remigio is the recipient of an Australian Government Research Training Program Scholarship at The University of Queensland, Australia. This work was supported by the French National Research Agency through the national program "Investissements d'avenir" (ANR-10-LABX-21 - RESSOURCES21).

AUTHOR CONTRIBUTIONS

PNN, ACR and AVDE designed and conducted the experiment. PNN collected the samples and undertook the chemical analysis of the samples. PNN and AVDE conducted the micro-XRF analysis. PNN, ACR and AVDE wrote the manuscript.

CONFLICTS OF INTEREST

The authors declare no conflicts of interest relevant to the content of this manuscript.

References

1. Abubakari, F., Nkrumah, P.N., Erskine, P.D., Brown, G.K., Fernando, D.R., Echevarria, G., van der Ent, A., (2021a) Manganese (hyper) accumulation within Australian *Denhamia* (Celastraceae): an assessment of the trait and manganese accumulation under controlled conditions. Plant and Soil 63: 205–223.

2. Abubakari, F., Nkrumah, P.N., Fernando, D.R., Brown, G.K., Erskine, P.D., Echevarria, G., van der Ent, A., (2021b) Incidence of hyperaccumulation and tissue-level distribution of manganese, cobalt and zinc in the genus *Gossia* (Myrtaceae). Metallomics 3(4): mfab008.
3. Abubakari F, Nkrumah PN, Fernando DR, Erskine PD, Echevarria G, van der Ent A. (2022) Manganese accumulation and tissue-level distribution in the Australian hyperaccumulator *Gossia bidwillii* (Myrtaceae). Tropical Plant Biology. https://doi.org/10.1007/s12042-021-09307-1.
4. Anderson CWN, Bhatti SM, Gardea-Torresdey J, Parsons J (2013) *In vivo* effect of copper and silver on synthesis of gold nanoparticales inside living plants. ACS Sustainable Chem Eng 1:640–648.
5. Anderson CWN, Brooks RR, Chiarucci A, LaCoste CJ, Leblanc M, Robinson BH, Simcock R, Stewart RB. (1999) Phytomining for nickel, thallium and gold. Journal of Geochemical Exploration 67:407–415.
6. Assunção A.G., Bookum W.M., Nelissen H.J., *et al.* (2003). Differential metal-specific tolerance and accumulation patterns among *Thlaspi caerulescens* populations originating from different soil types. New Phytologist 159:411–419.
7. Baker AJM, Brooks RR (1989) Terrestrial higher plantswhich hyperaccumulate metallic elements – a reviewof their distribution, ecology and phytochemistry. Biorecovery 1:81–126
8. Batianoff GN, Reeves RD, Specht RL. (1990) *Stackhousia tryonii* Bailey: a nickel-accumulating serpentine-endemic species of Central Queensland. Australian Journal of Botany 38:121–130.
9. Bidwell SD, Woodrow IE, Batianoff GN, Sommer-Knudsen J (2002) Hyperaccumulation of manganese in the rainforest tree *Austromyrtus bidwillii* (Myrtaceae) from Queensland, Australia. Funct Plant Biol 29:899–905.
10. Blamey FPC, Joyce DC, Edwards DG, Asher CJ. (1986) Role of trichomes in Sunflower tolerance to manganese toxicity. Plant and Soil 91:171–180.
11. Blamey FP, Hernandez-Soriano MC, Cheng M, Tang C, Paterson DJ, Lombi E, Wang WH, Scheckel KG, Kopittke PM. (2015) Synchrotron-based techniques shed light on mechanisms of plant sensitivity and tolerance to high manganese in the root environment. Plant Physiology 169:2006–2020.
12. Blamey FP, McKenna BA, Li C, Cheng M, Tang C, Jiang H, Howard DL, Paterson DJ, Kappen P, Wang P, Menzies NW. (2018) Manganese distribution and speciation help to explain the effects of silicate and phosphate on manganese toxicity in four crop species. New Phytologist 217:1146–1160.
13. Broadhurst CL, Tappero RV, Maugel TK, Erbe EF, Sparks DL, Chaney RL. (2009) Interaction of nickel and manganese in accumulation and localization in leaves of the Ni hyperaccumulators *Alyssum murale* and *Alyssum corsicum*. Plant and Soil 314:35–48.
14. Callahan DL, Hare DJ, Bishop DP, Doble PA, Roessner U. (2016) Elemental imaging of leaves from the metal hyperaccumulating plant *Noccaea caerulescens* shows different spatial distribution of Ni, Zn and Cd. RSC advances 6:2337–2344.
15. Chaney RL, Baklanov IA (2017) Phytoremediation and phytomining: status and promise. In: Cuypers A, Vangronsveld J (eds) Advances in botanical research, vol 83. Academic Press, pp 189–221.

16. Clemens S. (2017) How metal hyperaccumulating plants can advance Zn biofortification. Plant and Soil 411:111–120.
17. Creus PK, Sanislav IV, Dirks PH. (2021) Application of SfM-MVS for mining geology: Capture set-up and automated processing using the Dugald River Zn-Pb-Ag mine as a case study. Engineering Geology 293:106314.
18. Deng T-H-B., Cloquet C., Tang Y-T., *et al*. (2014). Nickel and zinc isotope fractionation in hyperaccumulating and nonaccumulating plants. Environmental Science & Technology 48:11926–11933.
19. do Nascimento CW, Hesterberg D, Tappero R. (2021) Imaging Zn and Ni distributions in leaves of different ages of the hyperaccumulator *Noccaea caerulescens* by synchrotron-based X-ray fluorescence. Journal of Hazardous Materials 408:124813.
20. Entwistle JA, Hursthouse AS, Reis PA, Stewart AG. (2019) Metalliferous mine dust: Human health impacts and the potential determinants of disease in mining communities. Current Pollution Reports 5(3):67–83.
21. Escarré J, Lefèbvre C, Raboyeau S, Dossantos A, Gruber W, Cleyet Marel JC, Frérot H, Noret N, Mahieu S, Collin C, van Oort F (2011) Heavy metal concentration survey in soils and plants of the Les Malines Mining District (Southern France): implications for soil restoration. Water, Air, Soil Pollut 216:485–504.
22. Escarré J, Lefèbvre C, Gruber W, Leblanc M, Lepart J, Rivière Y, Delay B. (2000) Zinc and cadmium hyperaccumulation by *Thlaspi caerulescens* from metalliferous and nonmetalliferous sites in the Mediterranean area: implications for phytoremediation. New Phytologist 145:429–437.
23. European Commission (2020) *Critical Raw Materials* (European Commission 2020) https://ec.europa.eu/growth/sectors/raw-materials/areas-specific-interest/critical-raw-materials_en. Accessed: 16 February 2022.
24. Fernando DR, Guymer G, Reeves RD, Woodrow IE, Baker AJ, Batianoff GN. (2009) Foliar Mn accumulation in eastern Australian herbarium specimens: prospecting for 'new' Mn hyperaccumulators and potential applications in taxonomy. Annals of Botany 103:931–939.
25. Forsyth B, Edraki M, Baumgartl T. (2015) The evolution of tailings seepage chemistry at one of Australia's largest and longest operating mines. In:10th International Conference on Acid Rock Drainage and Annual IMWA Conference. Gecamin Digital Publications, pp. 1–11.
26. Francesconi K, Visoottiviseth P, Sridokchan W, Goessler W. (2002) Arsenic species in an arsenic hyperaccumulating fern, *Pityrogramma calomelanos*: a potential phytoremediator of arsenic-contaminated soils. Science of the Total Environment 284:27–35.
27. Gonneau C, Genevois N, Frérot H, Sirguey C, Sterckeman T. (2014) Variation of trace metal accumulation, major nutrient uptake and growth parameters and their correlations in 22 populations of *Noccaea caerulescens*. Plant and Soil 384:271–287.
28. Grčman H, Velikonja-Bolta Š, Vodnik D, Kos B, Leštan D. (2001) EDTA enhanced heavy metal phytoextraction: metal accumulation, leaching and toxicity. Plant and Soil 235:105–114.

29. Harvey MA, Erskine PD, Harris HH, Brown GK, Pilon-Smits EA, Casey LW, Echevarria G, van der Ent A. (2020) Distribution and chemical form of selenium in *Neptunia amplexicaulis* from Central Queensland, Australia. Metallomics 12:514–527.
30. Huang L, Li X, Nguyen TA. (2015) Extremely high phosphate sorption capacity in Cu-Pb-Zn mine tailings. PLoS One 10:e0135364.
31. International Energy Agency (IEA) (2021) Net zero by 2050: A roadmap for the global energy sector (IEA, 2021) https://www.iea.org/reports/net-zero-by-2050. (Accessed on 15 February 2022).
32. Jowitt SM, Mudd GM, Thompson JF. (2020) Future availability of non-renewable metal resources and the influence of environmental, social, and governance conflicts on metal production. Communications Earth & Environment 1:1–8.
33. Küpper H, Lombi E, Zhao F-J, McGrath SP. 2000. Cellular compartmentation of cadmium and zinc in relation to other elements in the hyperaccumulator *Arabidopsis halleri*. Planta 212:75–84.
34. Küpper H, Zhao FJ, McGrath SP. (1999) Cellular compartmentation of zinc in leaves of the hyperaccumulator *Thlaspi caerulescens*. Plant Physiol 119:305–311
35. Leblanc M, Deram A, Robinson BH, Petit D, Brooks RR (1999) The phytomining and environmental significance of hyperaccumulation of thallium by *Iberis intermedia* from Southern France. Econ Geol 94:109–113.
36. Li C, Wang P, van der Ent A, *et al*. (2019) Absorption of foliar-applied Zn in sunflower (*Helianthus annuus*): importance of the cuticle, stomata and trichomes. Annals of Botany 123:57–68.
37. Li C, Wu J, Blamey FP, Wang L, Zhou L, Paterson DJ, van der Ent A, Fernández V, Lombi E, Wang Y, Kopittke PM. (2021) Non-glandular trichomes of sunflower are important in the absorption and translocation of foliar-applied Zn. Journal of Experimental Botany 72:5079–5092.
38. Lottermoser BG, Ashley PM, Munksgaard NC. (2008) Biogeochemistry of Pb–Zn gossans, northwest Queensland, Australia: implications for mineral exploration and mine site rehabilitation. Applied Geochemistry 23:723–742.
39. Meers E, Lesage E, Lamsal S, Hopgood M, Vervaeke P, Tack FM, Verloo MG. (2005) Enhanced phytoextraction: I. Effect of EDTA and citric acid on heavy metal mobility in a calcareous soil. International Journal of Phytoremediation 7:129–142.
40. Mudd GM. (2007) An analysis of historic production trends in Australian base metal mining. Ore Geology Reviews 32:227–261.
41. Mudd GM. (2020) Metals and elements needed to support future energy systems. Future Energy 1:711–726.
42. Mudd GM, Jowitt SM, Werner TT. (2017) The world's lead-zinc mineral resources: scarcity, data, issues and opportunities. Ore Geology Reviews 80:1160–1190.
43. Nkrumah PN, Baker AJM, Chaney RL, Erskine PD, Echevarria G, Morel JL, van der Ent A (2016) Current status and challenges in developing nickel phytomining: an agronomic perspective. Plant Soil 406:55–69.

44. Nkrumah PN, Echevarria G, Erskine PD, van der Ent A (2018) Phytomining: using plants to extract valuable metals from mineralised wastes and uneconomic resources. In: Extracting Innovations: Mining, Energy, and Technological Change in the Digital Age, Clifford MJ, Perrons RK, Ali SH, Grice TA (Eds.), CRC Press, pp. 313–324.
45. Nkrumah PN, Tisserand R, Chaney RL, Baker AJM, Morel JL, Goudon R, Erskine PD, Echevarria G, van der Ent A (2019) The first tropical 'metal farm': Some perspectives from field and pot experiments. J Geochem Explor 198:114–122.
46. Nkrumah PN, Chaney RL, Morel JL (2021) Agronomy of 'metal crops' used in agromining. In: Agromining: extracting unconventional resources from plants, Mineral Resource Reviews series, Van der Ent A, Echevarria G, Baker AJM, Morel JL (Eds.), Springer, Cham, pp. 23–46
47. Nkrumah PN, Echevarria G, Erskine PD, van der Ent A (2022) Farming for battery metals. Sci Tot Environ. https://doi.org/10.1016/j.scitotenv.2022.154092.
48. Nowack B, Schulin R, Robinson BH (2006) Critical assessment of chelant-enhanced metal phytoextraction. Environmental Science & Technology 40:5225–5232.
49. Pollard AJ, Stewart HL, Roberson CB. (2009) Manganese hyperaccumulation in *Phytolacca americana* L. from the Southeastern United States. Northeastern Naturalist 16:155–162.
50. Pošćić F, Fellet G, Vischi M, Casolo V, Schat H, Marchiol L. (2015) Variation in heavy metal accumulation and genetic diversity at a regional scale among metallicolous and non-metallicolous populations of the facultative metallophyte *Biscutella laevigata* subsp. *laevigata*. International Journal of Phytoremediation 17:464–475.
51. Purwadi I, Gei V, Echevarria G, Erskine PD, Mesjasz-Przybyłowicz J, Przybyłowicz WJ, van der Ent A. (2021) Tools for the discovery of hyperaccumulator plant species in the field and in the herbarium. In: Agromining: extracting unconventional resources from plants, Mineral Resource Reviews series, van der Ent A, Echevarria G, Baker AJM, Morel JL (Eds.), Springer, Cham, pp. 183–195.
52. Reeves RD (2006) Hyperaccumulation of trace elements by plants. In: Morel J-L, Echevarria G, Goncharova N (eds) Phytoremediation of metal-contaminated soils. Springer Netherlands, Dordrecht, pp 25–52
53. Reeves RD, Baker AJM, Jaffré T, Erskine PD, Echevarria G, van der Ent A (2018a) A global database for plants that hyperaccumulate metal and metalloid trace elements. New Phytol 218:407–411.
54. Reeves RD, Schwartz C, Morel JL, Edmondson J (2001) Distribution and metal-accumulating behavior of *Thlaspi caerulescens* and associated metallophytes in France. Int J Phytoremediation 3:145–172.
55. Reeves RD, van der Ent A, Baker AJM (2018b) Global distribution and ecology of hyperaccumulator plants. In: Van der Ent A, Echevarria G, Baker AJM, Morel JL (eds) Agromining: farming for metals: extracting unconventional resources using plants. Springer International Publishing, Cham, pp 75–92.

56. Sarret G, Willems G, Isaure MP, Marcus MA, Fakra SC, Frerot H, Pairis S, Geoffroy N, Manceau A, Saumitou-Laprade P. (2009) Zinc distribution and speciation in *Arabidopsis halleri* × *Arabidopsis lyrata* progenies presenting various zinc accumulation capacities. New Phytologist 184:581–95.
57. Schwartz C, Echevarria G, Morel JL (2003) Phytoextraction of cadmium with *Thlaspi caerulescens*. Plant Soil 249 (1):27-35
58. Severne B. (1974) Nickel accumulation by *Hybanthus floribundus*. Nature 248:807–808.
59. Spitz K, Trudinger J. (2019) Mining and the environment: from ore to metal. CRC Press; Aug 20.
60. Tang RH, Erskine PD, Echevarria G, van der Ent A. 2020. Biogeochemistry of metallophytes of the Zn-Pb-Cu Dugald River Mine Lode, Queensland, Australia. Journal of Chemical Ecology.
61. van der Ent A, Baker AJM, Reeves RD, Chaney RL, Anderson CWN, Meech JA, Erskine PD, Simonnot M-O, Vaughan J, Morel JL, Echevarria G, Fogliani B, Rongliang Q, Mulligan DR (2015) Agromining: farming for metals in the future? Environ Sci Technol 49 (8):4773–4780.
62. van der Ent A, Baker AJM, Reeves RD, Pollard AJ, Schat H (2013) Hyperaccumulators of metal and metalloid trace elements: facts and fiction. Plant Soil 362 (1):319–334.
63. van der Ent A, Callahan DL, Noller BN, Mesjasz-Przybylowicz J, Przybylowicz WJ, Barnabas A, Harris HH. (2017) Nickel biopathways in tropical nickel hyperaccumulating trees from Sabah (Malaysia). Scientific Reports 7:1–21.
64. van der Ent A, Ocenar A, Tisserand R, Sugau JB, Echevarria G, Erskine PD. (2019) Herbarium X-ray fluorescence screening for nickel, cobalt and manganese hyperaccumulator plants in the flora of Sabah (Malaysia, Borneo Island). Journal of Geochemical Exploration 202:49–58.
65. van der Ent A, Przybylowicz WJ, de Jonge MD, Harris HH, Ryan CG, Tylko G, Paterson DJ, Barnabas AD, Kopittke PM, Mesjasz-Przybylowicz J. (2018) X-ray elemental mapping techniques for elucidating the ecophysiology of hyperaccumulator plants. New Phytol 218:432–452.
66. van der Ent A, Casey LW, Blamey FP, Kopittke PM. (2020) Time-resolved laboratory micro-X-ray fluorescence reveals silicon distribution in relation to manganese toxicity in soybean and sunflower. Annals of Botany 126:331–341.
67. van der Ent A, Parbhakar-Fox A, Erskine PD. (2021) Treasure from trash: Mining critical metals from waste and unconventional sources. Science of The Total Environment 758:143673.
68. van der Zee L, Corzo Remigio A, Casey LW, Purwadi I, Yamjabok J, van der Ent A, Kootstra G, Aarts MGM. (2021) Quantification of spatial metal accumulation patterns in *Noccaea caerulescens* by X-ray fluorescence image processing for genetic studies. Plant Methods 17:86.
69. Wang Y, Kanipayor R, Brindle ID (2014) Rapid high-performance sample digestion for ICP determination by ColdBlock™ digestion: part 1 environmental samples. J Anal At Spectrom 29:162–168.
70. Williams PJ. (1998) Metalliferous economic geology of the Mt Isa eastern succession, Queensland. Australian Journal of Earth Sciences 45:329–341.

71. Xu, C., Dai, Q., Gaines, L., Hu, M., Tukker, A., Steubing, B. (2020) Future material demand for automotive lithium-based batteries. Commun. Mater. 1:1–10.
72. Xu, X., Shi, J., Chen, Y., Chen, X., Wang, H., Perera, A., (2006) Distribution and mobility of manganese in the hyperaccumulator plant *Phytolacca acinosa* Roxb. (Phytolaccaceae). Plant and Soil 285:323–331.
73. Zhao F, Lombi E, McGrath S. (2003) Assessing the potential for zinc and cadmium phytoremediation with the hyperaccumulator *Thlaspi caerulescens*. Plant and Soil 249:37–43.

Figures

Figure 1

The status of the cultivated plants at harvest, A-D: Mt Isa Mine substrate (A: *Noccaea caerulescens* only; B: *Biscutella laevigata* co-cultured with *N. caerulescens*; C: *B. laevigata* only; D: *B. laevigata* co-cultured with *Lupinus albus*) and E-H: Dugald River Mine substrate (E: *N. caerulescens* only; F: *B. laevigata* co-cultured with *N. caerulescens* G: *B. laevigata* only; H: *B. laevigata* co-cultured with *L. albus*). There were 16 plants per box and the plants were grown for 12 weeks.

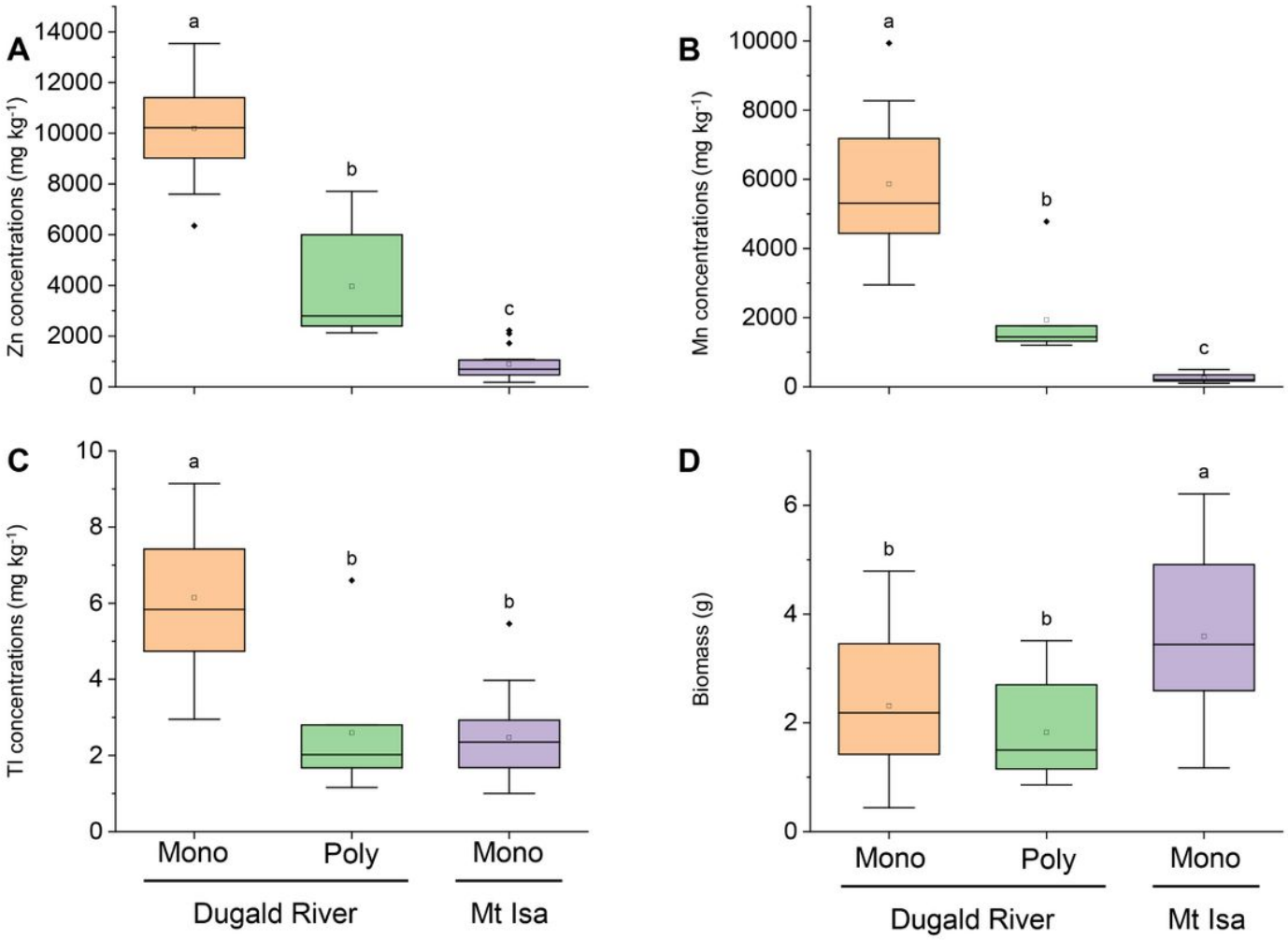

Figure 2

Elemental concentrations A) Zn, B) Mn and C) Tl, and D) shoot biomass of *Noccaea caerulescens* grown on the Dugald River Mine and Mt Isa Mine substrates (Mono: monoculture and Poly: co-cultured with *Biscutella laevigata*). Key to symbols of boxplots: open squares are the ± mean, whiskers are ± standard deviation (SD), circles are outliers. Mean ± standard error followed by the same letter are not significantly different (p >0.05) according to the Tukey test.

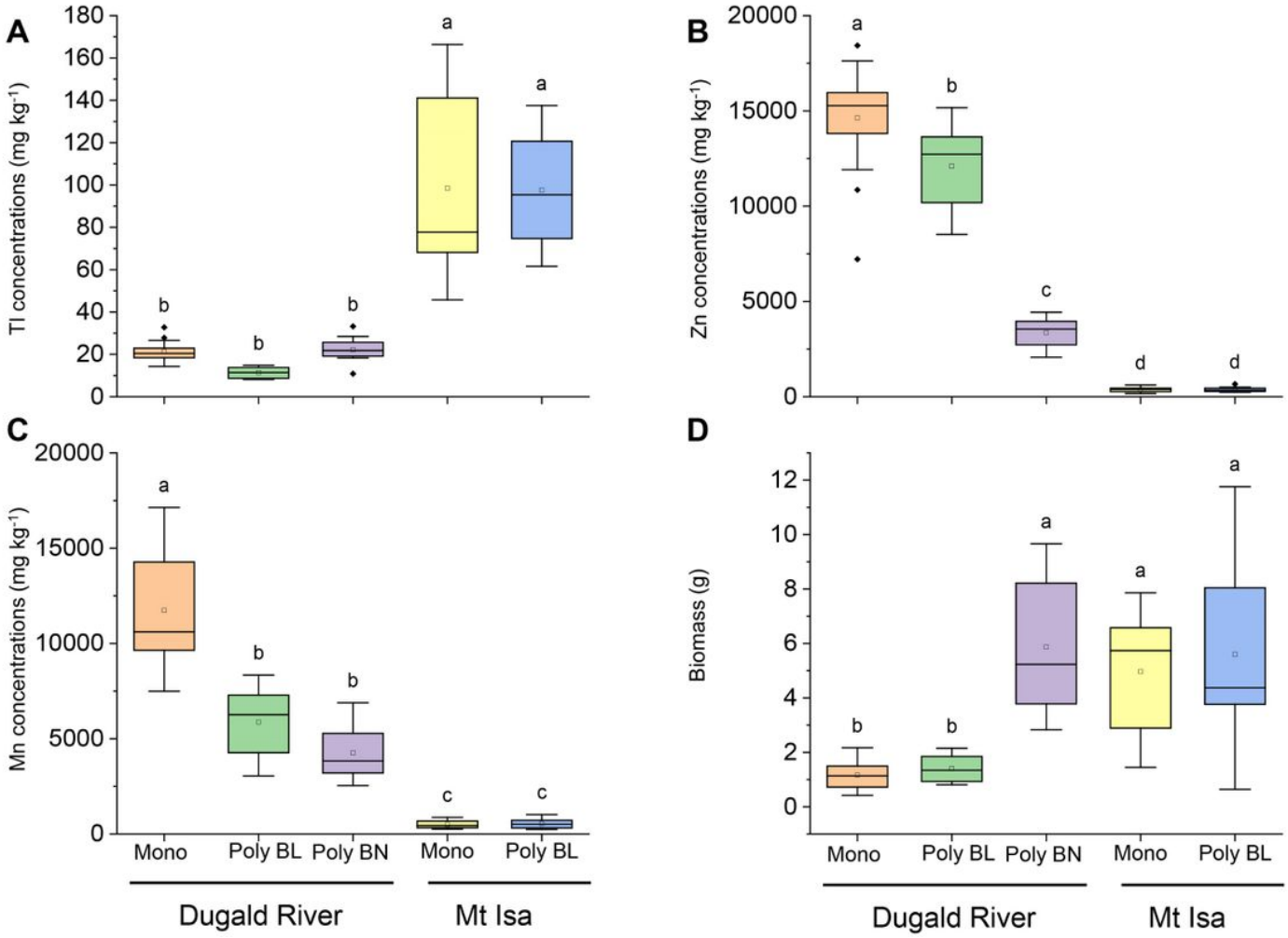

Figure 3

Elemental concentrations A) Tl, B) Zn and C) Mn, and D) shoot biomass of *Biscutella laevigata* grown on the Dugald River Mine and Mt Isa Mine substrates (Mono: monoculture, Poly BL: co-cultured with *Lupinus albus*, Poly BN: co-cultured with *Noccaea caerulescens*). Key to symbols of boxplots: open squares are the ± mean, whiskers are ± standard deviation (SD), circles are outliers. Mean ± standard error followed by the same letter are not significantly different (p >0.05) according to the Tukey test.

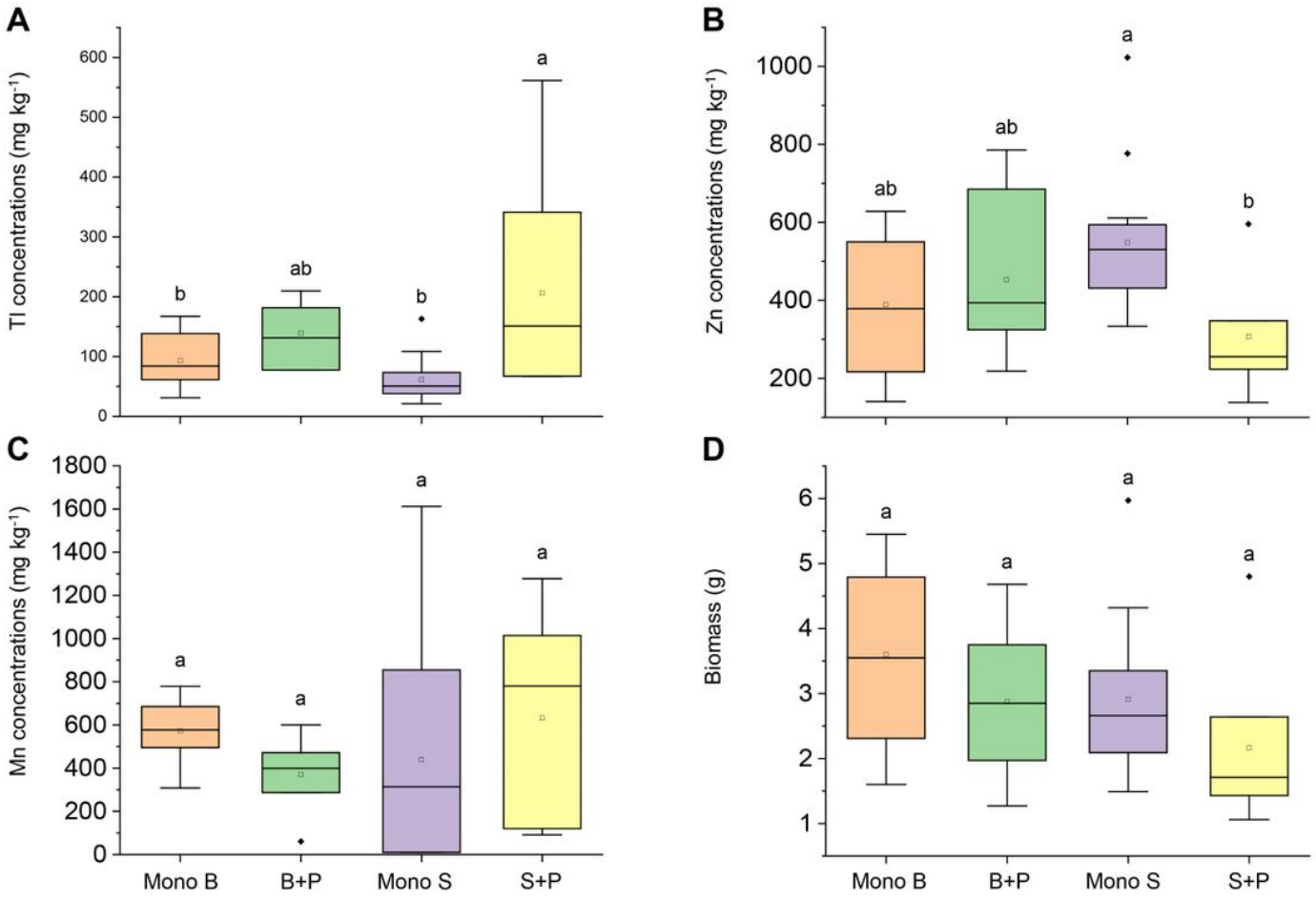

Figure 4

Elemental concentrations A) Tl, B) Zn and C) Mn, and D) shoot biomass of *Biscutella laevigata* and *Silene latifolia* grown on the Mt Isa Mine substrate (Mono B: monoculture *B. laevigata*, B+P: *B. laevigata* co-cultured with *Phytolacca octandra*, P Mono S: monoculture *S. latifolia*, S+P: *S. latifolia* co-cultured with *P. octandra*). Key to symbols of boxplots: open squares are the ± mean, whiskers are ± standard deviation (SD), circles are outliers. Mean ± standard error followed by the same letter are not significantly different (p >0.05) according to the Tukey test.

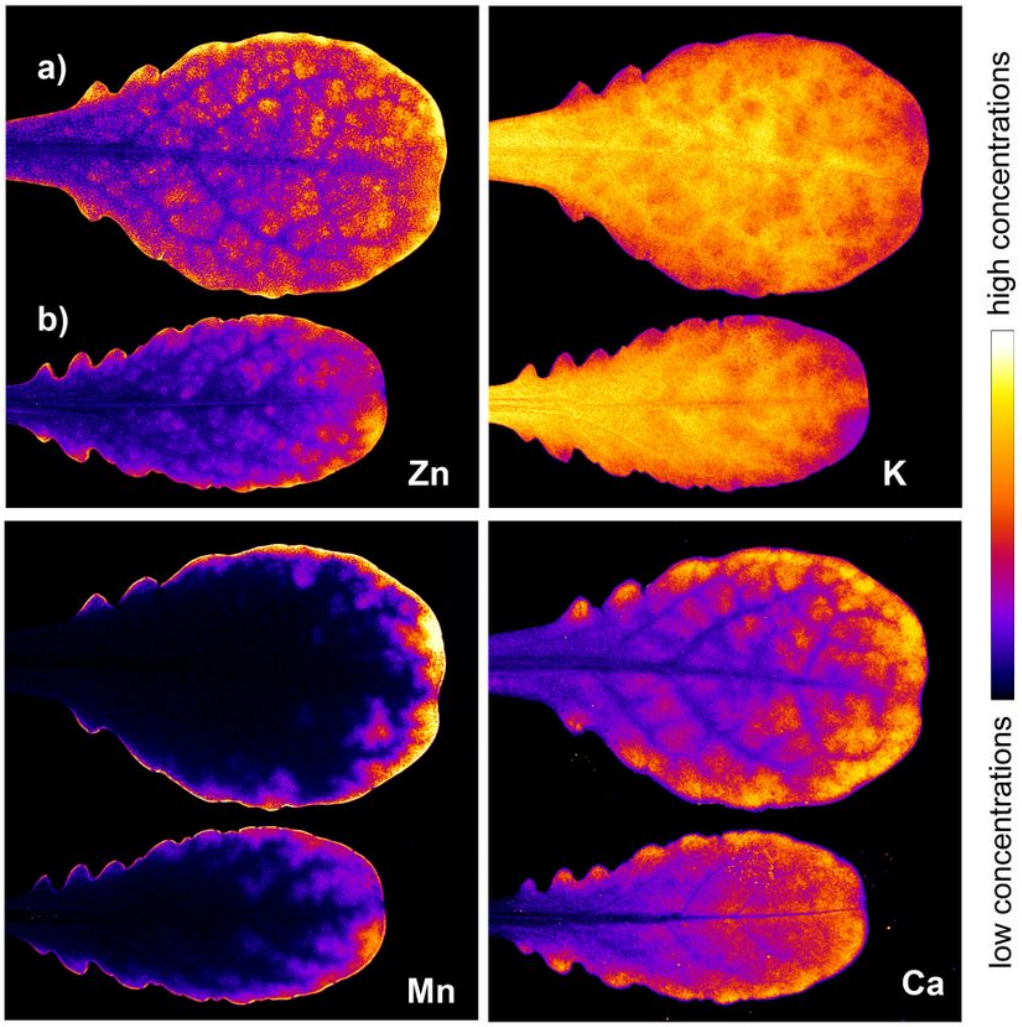

Figure 5

Laboratory micro-X-ray fluorescence (μXRF) maps of Zn, Mn, K and Ca of hydrated leaves of *Noccaea caerulescens* (monoculture) grown on the a) Dugald River Mine substrate and b) Mt Isa Mine substrate.

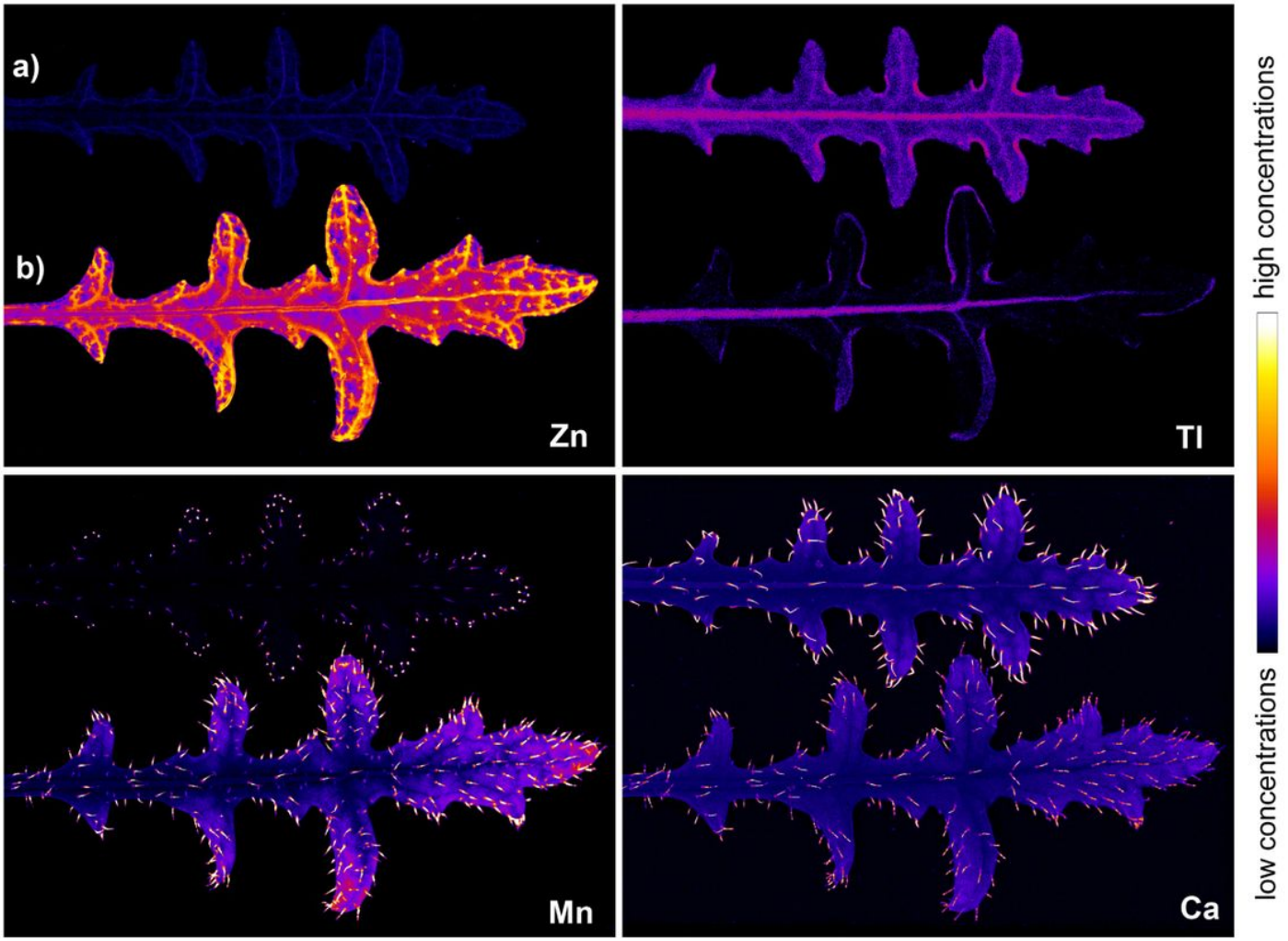

Figure 6

Laboratory micro-X-ray fluorescence (μXRF) maps of Zn, Mn, Tl and Ca of hydrated leaves of *Biscutella laevigata* (monoculture) grown on the a) Mt Isa Mine substrate and b) Dugald River Mine substrate.

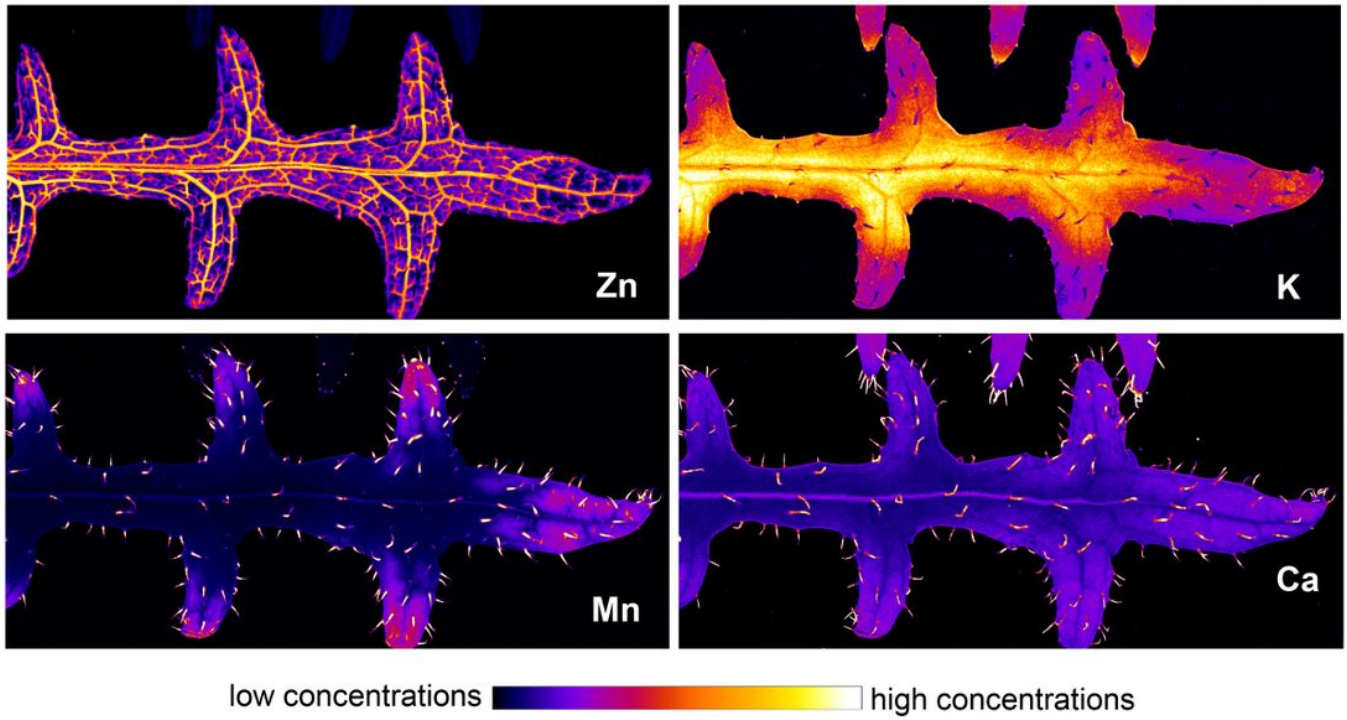

Figure 7

Laboratory micro-X-ray fluorescence (μXRF) maps of Zn, Mn, K and Ca of hydrated leaves of *Biscutella laevigata* co-cultured with *Noccaea caerulescens* on the Dugald River Mine substrate.

Figure 8

Laboratory micro-X-ray fluorescence (μXRF) maps of Zn, Mn, K and Ca of hydrated leaves of *Phytolacca octandra* grown on the Mt Isa Mine substrate.

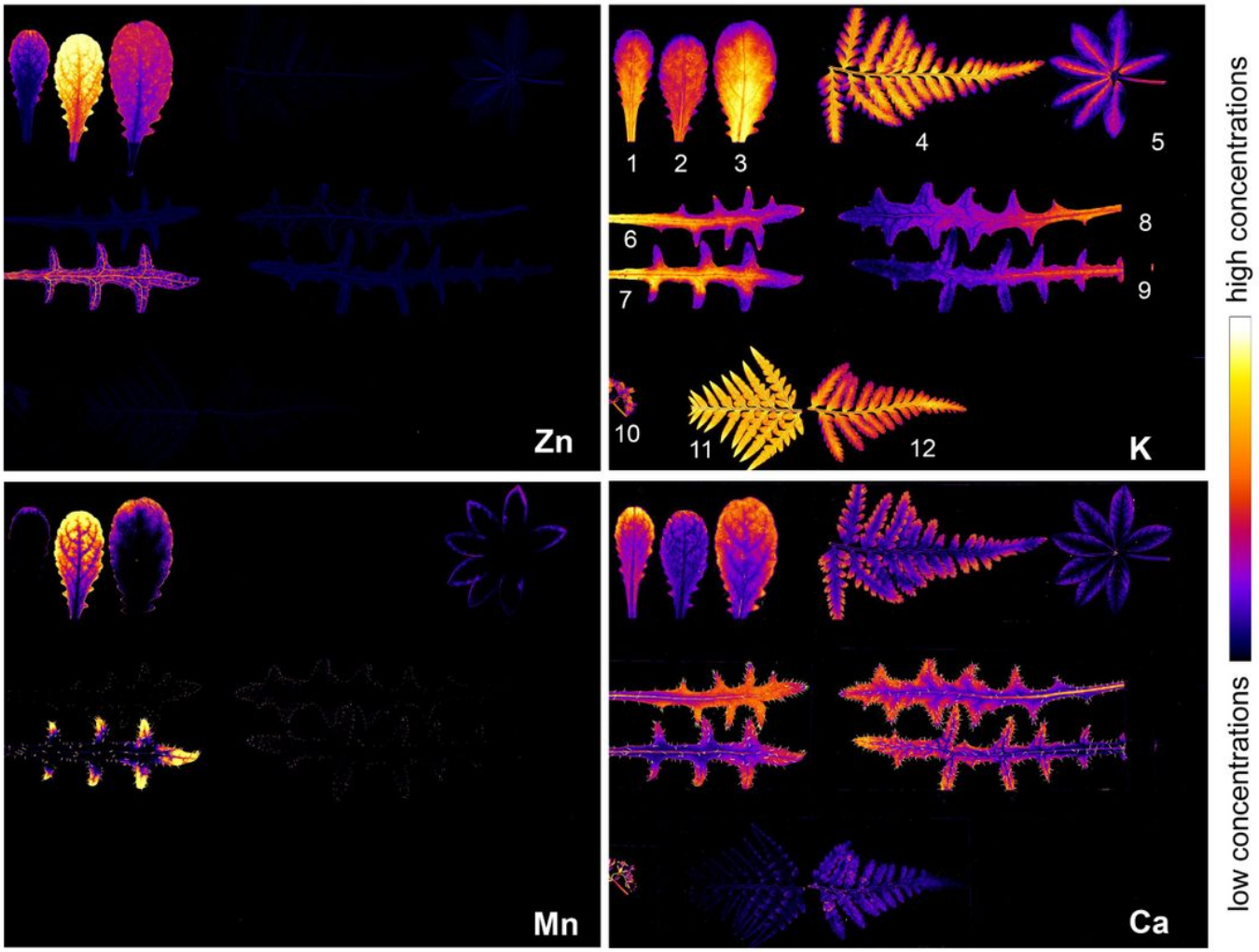

Figure 9

Laboratory micro-X-ray fluorescence (μXRF) maps of Zn, Mn, K and Ca of hydrated leaves of 1) *Noccaea caerulescens* only on Mt Isa Mine substrate; 2) *Noccaea caerulescens* only on Dugald River Mine substrate; 3) *Noccaea caerulescens* co-cultured with *Biscutella laevigata* on Dugald River Mine substrate; 4, 11, 12) *Pityrogramma calomelanos* co-cultured with *B. laevigata* on Mt Isa Mine substrate; 5) *Lupinus albus* co-cultured with *B. laevigata* on Mt Isa Mine substrate; 6) *Biscutella laevigata* co-cultured with *P. calomelanos* on Mt Isa Mine substrate; 7) *Biscutella laevigata* co-cultured with *N. caerulescens* on Mt Isa Mine substrate; 8) *Biscutella laevigata* only on Mt Isa Mine substrate; 9) *Biscutella laevigata* only on Dugald River Mine substrate; 10) *Biscutella laevigata* (flower) on Mt Isa Mine substrate.